TDOA Based Positioning in the Presence of Unknown Clock Skew

Mohammad Reza Gholami, *Student Member, IEEE*,
Sinan Gezici, *Senior Member, IEEE*, and Erik G. Ström, *Senior Member, IEEE*

***Abstract*—This paper studies the positioning problem of a single target node based on time-difference-of-arrival (TDOA) measurements in the presence of clock imperfections. Employing an affine model for the behaviour of a local clock, it is observed that TDOA based approaches suffer from a parameter of the model, called the clock skew. Modeling the clock skew as a nuisance parameter, this paper investigates joint clock skew and position estimation. The maximum likelihood estimator (MLE) is derived for this problem, which is highly nonconvex and difficult to solve. To avoid the difficulty in solving the MLE, we employ suitable approximations and relaxations and propose two suboptimal estimators based on semidefinite programming and linear estimation. To further improve the estimation accuracy, we also propose a refining step. In addition, the Cramér-Rao lower bound (CRLB) is derived for this problem as a benchmark. Simulation results show that the proposed suboptimal estimators can attain the CRLB for sufficiently high signal-to-noise ratios.**

***Index Terms*—Wireless sensor network, time-difference-of-arrival (TDOA), clock skew, semidefinite programming, linear estimator, maximum likelihood estimator (MLE), Cramér-Rao lower bound (CRLB), positioning, clock synchronization.**

I. INTRODUCTION

POSITIONING of sensor nodes based on time-of-arrival (TOA) measurements is a popular technique for wireless sensor networks (WSNs) [1]–[6]. TOA-based positioning can potentially provide highly accurate estimation of target's position in some situations, e.g., in line-of-sight conditions and for sufficiently high signal-to-noise ratios (SNRs) [1], [7]. Despite its high performance, TOA-based positioning is strongly affected by the clock offset imperfection, a fixed deviation from a reference clock at time zero. To resolve this problem, time-difference-of-arrival (TDOA) based positioning has been proposed as an alternative approach in the literature [1], [2], [8], which has found various applications in practice, e.g., in the Global Positioning System.

Manuscript received June 5, 2012; revised December 5, 2012 and January 25, 2013. The associate editor coordinating the review of this paper and approving it for publication was E. Serpedin.

M. R. Gholami and E. G. Ström are with the Division of Communication Systems, Information Theory, and Antennas, Department of Signals and Systems, Chalmers University of Technology, SE-412 96 Gothenburg, Sweden (e-mail: {moreza, erik.strom}@chalmers.se).

S. Gezici is with the Department of Electrical and Electronics Engineering, Bilkent University, Ankara 06800, Turkey (e-mail: gezici@ee.bilkent.edu.tr).

This work was supported in part by the European Commission in the framework of the FP7 Network of Excellence in Wireless COMmunications # (contract no. 318306), in part by the Swedish Research Council (contract no. 2007-6363), and in part by Turk Telekom (contract no. 3015-02).

Digital Object Identifier 10.1109/TCOMM.2013.032013.120381

The clock of an oscillator can be described via an affine model, which involves the clock offset and clock skew parameters [9]. While the clock offset corresponds to a fixed time offset due to clock imperfections, the clock skew parameter defines the rate of variations in the local clock compared to the real time [10], [11]. While the TDOA technique resolves the clock offset ambiguity, it can still suffer from the clock skew. It means that the actual difference between two TOAs, which forms a TDOA measurement, in a target node might be larger or smaller than the actual difference even in the absence of the measurement noise. For an ideal clock, the clock skew is equal to one and it might be larger or smaller than one for an unsynchronized clock. Thus, a position estimate may be considerably affected by a non-ideal clock skew for an unsynchronized network in practical scenarios, depending on how much the clock skew deviates from one.

During the last few years, various synchronization techniques have been proposed in the literature; e.g., see [10]–[13] and references therein. While traditionally synchronization and positioning are separately studied in MAC and physical layers, respectively, the authors in [14] formulate a joint synchronization and positioning problem in the MAC layer. If the major delay is the fixed delay due to propagation through the radio channel, the joint position and timing estimation technique works well. The method developed in [14] is based on a two-way message passing protocol that can be considered as a counterpart to two-way TOA ranging in the physical layer [15]. The authors in [7] investigate the positioning problem based on time of flight measurements for asynchronous networks in the physical layer and propose a technique based on the linear least squares. Using approximations, the authors in [16]–[18] propose differential TDOA to mitigate the effects of imperfect clock impairments. This method can cause noise enhancement and performance degradation in some scenarios. Such an approach is effective when only clock offsets exist in target and reference nodes and when there are more than one target node. In addition, the proposed iterative method based on a nonlinear least squares criterion may converge to a local minimum resulting in a large positioning error since the objective function is nonconvex.

In this paper, we study the single node positioning problem in the physical layer for one way ranging, where an unsynchronized target node tries to find its position by computing TDOA measurements (self-positioning). We assume that a number of reference nodes are perfectly synchronized with a reference clock and transmit their signals at a common time instant.[1] Then, the target node measures the TOAs of the received signals and forms a set of the TDOA measurements. By constructing a TDOA measurement, the clock offset vanishes in the TDOA measurement, but, as mentioned previously, an unsynchronized clock skew still affects the TDOA measurements. Since the clock skew is unknown, in this study, we consider it as a nuisance parameter and involve it in the position estimation. In fact, we deal with the joint estimation of the clock skew and the position of the target node. Note that we consider a fixed clock skew during the TDOA measurements since its variations during a period of time is assumed to be negligible. For Gaussian measurement errors, the maximum likelihood estimator (MLE) for this problem is highly nonconvex and difficult to solve. In order to derive a computationally efficient algorithm, we consider a number of approximations and relaxations, and propose two suboptimal estimators, which can be efficiently solved to provide coarse position estimates. The first estimator is based on relaxing the nonconvex problem to a semidefinite programming (SDP). Using a linearization technique, we derive a linear model and consequently apply a linear least squares (LLS) approach to find an estimate of the target position. We, then, apply a correction technique [19] to improve the estimation accuracy. In order to improve the accuracy of the coarse estimate provided by the SDP or the LLS, we linearize the measurements using the first-order Taylor series expansion around the estimate and obtain a linear model in which the estimation error can be approximated. Based on that model, the coarse position estimate can be further improved. To compare different approaches, we derive the Cramér-Rao lower bound (CRLB) as a benchmark. We also study the CRLB when an estimate of the clock skew is available (through simulations) and investigate the effectiveness of the proposed approaches.

In summary, the *main contributions* of this work are:

1) the idea of joint clock skew and position estimation based on TDOA measurements;
2) derivation of the MLE and the CRLB for the problem considered in this study;
3) deriving two suboptimal estimators to provide coarse estimates of the target location based on linearization and relaxation techniques;
4) proposing a simple estimator based on the first order Taylor-series expansion around the coarse estimate to obtain a refined position estimate.

The remainder of the paper is organized as follows. Section II explains the signal model considered in this paper. In Section III, the maximum likelihood estimator and a theoretical lower bound are derived for the problem. Two suboptimal estimators are studied in Section IV. Simulation results are discussed in Section V. Finally, Section VI makes come concluding remarks.

Notation: The following notations are used in this paper. Lowercase and bold lowercase letters denote scalar values and vectors, respectively. Matrices are written in bold uppercase letters. $\mathbf{1}_M$ and $\mathbf{0}$ denote the vector of M ones and the vector (matrix) of all zeros, respectively. $\mathbf{I}_M$ is an M by M identity matrix. The operators $\mathrm{tr}(\cdot)$ and $\mathbb{E}\{\cdot\}$ are used to denote the trace of a square matrix and the expectation of a vector (variable), respectively. The Euclidian norm of a vector is denoted by $\|\cdot\|$. The $(\mathrm{blk})\mathrm{diag}(X_1,\ldots,X_N)$ is a (block) diagonal matrix with diagonal elements (blocks) $X_1,\ldots,X_N$. $d(\mathbf{a},\mathbf{b}) = \|\mathbf{a}-\mathbf{b}\|$ is the distance between $\mathbf{a}$ and $\mathbf{b}$, and $\otimes$ denotes the Kronecker product. Given two matrices $\mathbf{A}$ and $\mathbf{B}$, $\mathbf{A} \succeq \mathbf{B}$ means that $\mathbf{A}-\mathbf{B}$ is positive semidefinite. $\mathbb{S}^m$ and $\mathbb{R}^m_+$ denote the set of all $m \times m$ symmetric matrices and the set of all $m \times 1$ vectors with positive elements, respectively. $[\mathbf{A}]_{i,j}$ denotes the element of matrix $\mathbf{A}$ in the ith row and the jth column.

[1]Another alternative is to measure TOAs of the signal transmitted by a target node in the reference nodes and then to transfer the measurements to a central unit to compute the TDOAs, from which the position of the target is estimated (remote positioning). Although this method can resolve the clock imperfection of the target node, it needs a central processing unit and requires that the final estimate should be sent back to the target node.

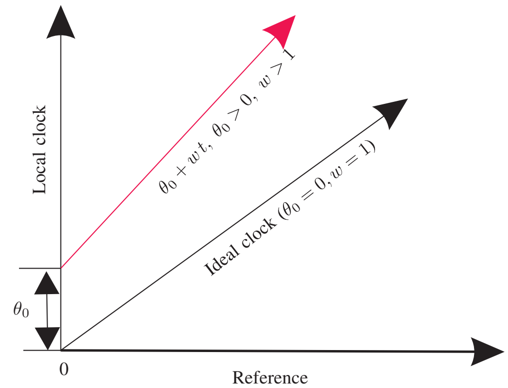

Fig. 1. Local clock versus real clock.

II. System Model

Consider a two-dimensional (2-D) network[2] with $N+1$ sensor nodes. Suppose that the first N sensors are reference (anchor) nodes which are located at known positions $\mathbf{a}_i = [a_{i,1}\ a_{i,2}]^T \in \mathbb{R}^2$, $i = 1,...,N$, and the last sensor node is the target node which is placed at unknown position $\mathbf{x} = [x_1\ x_2]^T \in \mathbb{R}^2$. It is assumed that the reference nodes are synchronized with a reference clock while the clock of the target node is left unsynchronized. The following affine model is employed for the local clock of the target node [10]:

$$C(t) = \theta_0 + w\,t\ , \tag{1}$$

where θ_0 and w denote, respectively, the relative clock offset and the clock skew between the target node and the reference time t.

To get some insight into this model, consider Fig. 1, which illustrates the relation between a local clock and a real clock. For the example in the figure, the local time varies faster than the ideal time, i.e., $w > 1$. The affine model for the clock is a common model and has been justified in the literature, e.g., see [9], [10], [20] and references therein. Therefore, this model is employed throughout the paper. Assume that the target node is able to measure the TOAs of the received signals from

[2]The generalization to a three-dimensional scenario is straightforward, but is not explored in this paper.

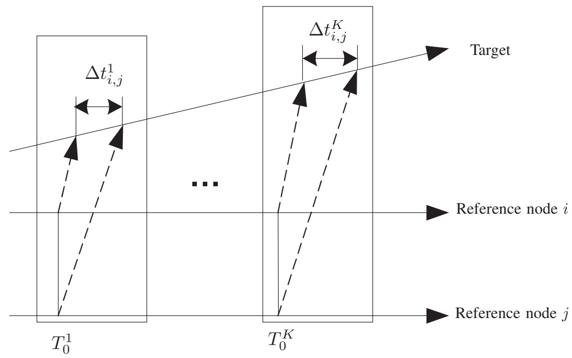

Fig. 2. TDOA measurement at the target node for signals from two reference nodes i and j.

the reference nodes. Suppose that the synchronized reference nodes send their signals at the time instant T_0^k (see Fig. 2). The TOA measurement for the signal transmitted from reference node i at the target node for the kth measurement can be written[3] as [21], [22]

$$t_i^k = \theta_0 + w\left(T_0^k + \frac{d(\mathbf{a}_i, \mathbf{x})}{c}\right) + \tilde{n}_i^k, \quad i = 1, \ldots, N, \quad k = 1, \ldots, K, \tag{2}$$

where c is the speed of propagation, $d(\mathbf{a}_i, \mathbf{x})$ is the Euclidian distance between reference node i and the point $\mathbf{x}$, $\tilde{n}_i^k$ is the TOA estimation error at the target node for the signal transmitted from the ith reference node at time T_0^k, and K is the number of TOA measurements (messages) for every link between a reference node and the target node (collected in the target node). The estimation error is often modeled by a zero-mean Gaussian random variable with variance σ_i^2/c^2; i.e., $\tilde{n}_i^k \sim \mathcal{N}(0, \sigma_i^2/c^2)$ [4], [5]. In addition, it is assumed that $\mathbb{E}\{\tilde{n}_i^l \, \tilde{n}_j^m\} = 0$ for $i \neq j$ or $l \neq m$. Note that we assume that θ_0 and w are fixed unknown parameters for $k = 1, \ldots, K$.

The preceding measurement model indicates that in order to obtain an estimate of the distance between the target node and a reference node, parameters θ_0, w, and T_0^k (as nuisance parameters) should be estimated as well. For instance, the measurements in (2) can be collected by the target node to derive an optimal estimator for estimating the unknown parameters including the nuisance parameters, which makes the problem quite complex and challenging. One way to get rid of some of the unknown parameters is to subtract TOA measurements of the signals sent from reference nodes i and j, and form a TDOA measurement as follows:

$$\Delta t_{i,j}^k = t_i^k - t_j^k = w\left(\frac{d(\mathbf{a}_i, \mathbf{x})}{c} - \frac{d(\mathbf{a}_j, \mathbf{x})}{c}\right) + \tilde{n}_i^k - \tilde{n}_j^k, \quad i \neq j = 1, \ldots, N. \tag{3}$$

As observed from (3), the clock offset θ_0 and T_0^k have no effect on TDOA measurements since they cancel out in the TDOA calculation. The clock skew, however, still affects the TDOA measurements and it should be considered when estimating the target node position. Throughout this paper, we assume that the TDOA measurements are computed by subtracting all the TOA measurements, except the first one, from the first TOA. Consequently, the range-difference-of-arrival (RDOA) measurements are obtained as

$$z_{i,1}^k = c\Delta t_{i,1}^k = w\, d_{i,1} + n_i^k - n_1^k, \quad i = 2, \ldots, N, \quad k = 1, \ldots, K, \tag{4}$$

where $n_i^k = c\,\tilde{n}_i^k$ and $d_{i,1} = d(\mathbf{a}_i, \mathbf{x}) - d(\mathbf{a}_1, \mathbf{x})$.

Define the vector of measurements $\mathbf{z}$ as

$$\mathbf{z} = \left[\mathbf{z}_1^T \ \cdots \ \mathbf{z}_K^T\right]^T \in \mathbb{R}^{K(N-1)}, \tag{5}$$

where

$$\mathbf{z}_k = \left[z_{2,1}^k \ \ldots \ z_{N,1}^k\right]^T \in \mathbb{R}^{(N-1)}. \tag{6}$$

In order to find the position of the target node based on the measurements in (5), one needs to estimate the clock skew w as well.

III. Maximum Likelihood Estimator and Theoretical Limits

In this section, we first derive the MLE for the positioning problem based on the measurements in (4)–(6). In the sequel we obtain a theoretical lower bound on the variance of any unbiased estimator. Note that the estimator obtained in this section is optimal for the new set of measurements in (5) and not necessarily optimal for the original TOA measurements in (2).

A. Maximum Likelihood Estimator (MLE)

To find the MLE, we need to solve the following optimization problem [23, Ch. 7]:

$$[\hat{\mathbf{x}}^T \ \hat{w}] = \underset{[\mathbf{x}^T \ w] \in \mathbb{R}^3}{\arg\max} \ p_{\mathbf{Z}}(\mathbf{z}; \mathbf{x}, w) \ , \tag{7}$$

where $p_{\mathbf{Z}}(\mathbf{z}; \mathbf{x}, w)$ is the probability density function of vector $\mathbf{z}$, which is indexed by parameters $\mathbf{x}$ and w. Since the TOA errors are Gaussian random variables, $\mathbf{z}$ in (5) is modeled as a Gaussian random vector, i.e., $\mathbf{z} \sim \mathcal{N}(\boldsymbol{\mu}_K, \mathbf{C}_K)$, with mean $\boldsymbol{\mu}_k$ and covariance matrix $\mathbf{C}_K$ being computed as follows:

$$\boldsymbol{\mu}_K = \mathbf{1}_K \otimes \boldsymbol{\mu} \in \mathbb{R}^{K(N-1)}, \quad \mathbf{C}_K = \text{blkdiag}\Big(\underbrace{\mathbf{C}, \ldots, \mathbf{C}}_{K \text{ times}}\Big) \in \mathbb{R}^{K(N-1)\times K(N-1)}, \tag{8}$$

where

$$\boldsymbol{\mu} = w\left[d_{2,1} \ \ldots \ d_{N,1}\right]^T, \quad \mathbf{C} = \text{diag}(\sigma_2^2, \ldots, \sigma_N^2) + \sigma_1^2 \mathbf{1}_{N-1}\mathbf{1}_{N-1}^T. \tag{9}$$

Therefore considering the model in (4), the MLE formulation can be expressed as

$$[\hat{\mathbf{x}}^T \ \hat{w}] = \underset{[\mathbf{x}^T \ w] \in \mathbb{R}^3}{\arg\min} \left[\mathbf{z} - \boldsymbol{\mu}_K\right]^T \mathbf{C}_K^{-1} \left[\mathbf{z} - \boldsymbol{\mu}_K\right]. \tag{10}$$

Using Woodbury's identity [24], which is a special case of the matrix inversion lemma, one can write

$$\mathbf{C}^{-1} = \text{diag}\left(\sigma_2^{-2}, \ldots, \sigma_N^{-2}\right) - s\,\text{diag}\left(\sigma_2^{-2}, \ldots, \sigma_N^{-2}\right) \mathbf{1}_{N-1}\mathbf{1}_{N-1}^T \text{diag}\left(\sigma_2^{-2}, \ldots, \sigma_N^{-2}\right). \tag{11}$$

[3] If time stamping is performed in the MAC layer, a model including fixed and random delays with no measurement noise can be considered. Such a model has been extensively studied in the synchronisation literature, e.g., in [10] and references therein.

where $s \triangleq 1/(\sum_{i=1}^{N} \sigma_i^{-2})$.

Then, the MLE can be obtained as

$$[\hat{\mathbf{x}}^T \;\; \hat{w}] = \underset{[\mathbf{x}^T \;\; w]\in\mathbb{R}^3}{\arg\min} \sum_{k=1}^{K}\sum_{i=2}^{N}\Bigg(\Big(\frac{z_{i,1}^k - w\, d_{i,1}}{\sigma_i}\Big)^2 - s\sum_{j=2}^{N}\frac{(z_{i,1}^k - w\, d_{i,1})(z_{j,1}^k - w\, d_{j,1})}{\sigma_i^2\sigma_j^2}\Bigg). \quad (12)$$

As observed from (12), the MLE problem is highly nonconvex and therefore is difficult to solve. To obtain the solution of this problem, a grid search approach or an iterative search, e.g., gradient-based approach, initialized close to the target position and close to the clock skew can be used. A grid search method has some drawbacks such as complexity. Moreover, finding a good initial point in the positioning problem is often a challenging task [21]. In Section IV, we derive suboptimal estimators to find good initial points. Before the detailed discussions on these suboptimal estimators in Section IV, the CRLBs are obtained in the following subsection in order to provide performance benchmarks.

B. Cramér-Rao Lower Bound (CRLB)

Considering the measurement vector in (5) with mean $\boldsymbol{\mu}_K$ and covariance matrix $\mathbf{C}_K$ as in (8), the elements of the Fisher information matrix can be computed as [23, Ch. 3]

$$J_{nm} = [\mathbf{J}]_{nm} = \left[\frac{\partial \boldsymbol{\mu}_K}{\partial \psi_n}\right]^T \mathbf{C}_K^{-1}\left[\frac{\partial \boldsymbol{\mu}_K}{\partial \psi_m}\right], \quad n, m = 1, 2, 3, \quad (13)$$

where

$$\psi_n = \begin{cases} x_n, & \text{if } n = 1, 2 \\ w, & \text{if } n = 3. \end{cases} \quad (14)$$

From (9), $\partial \boldsymbol{\mu}_K / \partial \psi_n$ can be obtained as follows:

$$\left[\frac{\partial \boldsymbol{\mu}_K}{\partial \psi_n}\right] = \mathbf{1}_K \otimes \left[\frac{\partial \mu_1}{\partial \psi_n} \;\; \dots \;\; \frac{\partial \mu_{N-1}}{\partial \psi_n}\right]^T, \quad n = 1, 2, 3, \quad (15)$$

where

$$\frac{\partial \mu_i}{\partial \psi_n} = \begin{cases} w\left(\frac{x_n - a_{i+1,n}}{d(\mathbf{a}_{i+1},\mathbf{x})} - \frac{x_n - a_{1,n}}{d(\mathbf{a}_1,\mathbf{x})}\right), & \text{if } n = 1, 2 \\ d_{i+1,1}, & \text{if } n = 3. \end{cases} \quad (16)$$

After some calculations, the entries of the Fisher information matrix can be computed as follows:

$$\begin{aligned} J_{11} &= Kw^2 \sum_{i=2}^{N}\left(I_{i,1}^2 - sI_{i,1}\bar{I}_{i,1}\right), \\ J_{22} &= Kw^2 \sum_{i=2}^{N}\left(I_{i,2}^2 - sI_{i,2}\bar{I}_{i,2}\right), \\ J_{33} &= K\sum_{i=2}^{N}\Big(\frac{d_{i,1}^2}{\sigma_i^2} - s\sum_{j=2}^{N}\frac{d_{i,1}d_{j,1}}{\sigma_i^2\sigma_j^2}\Big), \\ J_{12} = J_{21} &= Kw^2 \sum_{i=2}^{N}\left(I_{i,1}I_{i,2} - sI_{i,2}\bar{I}_{i,1}\right), \\ J_{13} = J_{31} &= Kw \sum_{i=2}^{N}\left(I_{i,1}d_{i,1} - \frac{s}{\sigma_i}\bar{I}_{i,1}d_{i,1}\right), \\ J_{23} = J_{32} &= Kw \sum_{i=2}^{N}\left(I_{i,2}d_{i,1} - \frac{s}{\sigma_i}\bar{I}_{i,2}d_{i,1}\right) \end{aligned} \quad (17)$$

where

$$\begin{aligned} I_{i,n} &= \frac{1}{\sigma_i}\left(\frac{x_n - a_{i,n}}{d(\mathbf{a}_i,\mathbf{x})} - \frac{x_n - a_{1,n}}{d(\mathbf{a}_1,\mathbf{x})}\right), \\ \bar{I}_{i,n} &= \sum_{l=2}^{N}\frac{1}{\sigma_l^2\sigma_i}\left(\frac{x_n - a_{l,n}}{d(\mathbf{a}_l,\mathbf{x})} - \frac{x_n - a_{1,n}}{d(\mathbf{a}_1,\mathbf{x})}\right). \end{aligned} \quad (18)$$

The CRLB, which is a lower bound on the variance of any unbiased estimator, is given as

$$\mathrm{Var}(\hat{\phi}_i) \ge [\mathbf{J}^{-1}]_{i,i}\,. \quad (19)$$

Then, the lower bounds on the error variances for any unbiased estimates of the position and the clock skew can be computed as (using the inverse of a 3×3 square matrix [24])

$$\mathbb{E}\{\|\hat{\mathbf{x}} - \mathbf{x}\|^2\} \ge \frac{J_{33}(J_{22} + J_{11}) - (J_{32}^2 + J_{13}^2)}{J_{33}(J_{11}J_{22} - J_{12}^2) + (2J_{31}J_{23}J_{12} - J_{22}J_{13}^2 - J_{11}J_{23}^2)}, \quad (20a)$$

$$\mathbb{E}\{\|\hat{w} - w\|^2\} \ge \frac{J_{11}J_{22} - J_{12}^2}{J_{33}(J_{11}J_{22} - J_{12}^2) + (2J_{31}J_{23}J_{12} - J_{22}J_{13}^2 - J_{11}J_{23}^2)}. \quad (20b)$$

In the rest of this section, we derive an alternative CRLB for position estimation when an estimate of the clock skew is available. To that aim, we model the clock skew estimate as a Gaussian random variable $\hat{w} = w + \xi_w$, where ξ_w is the error in the clock skew estimation that is modeled as a zero-mean Gaussian random variable, $\xi_w \sim \mathcal{N}(0, \sigma_w^2)$, and rewrite (4) as

$$\bar{z}_{i,1}^k = \hat{w}\, d_{i,1} - \xi_w\, d_{i,1} + n_i^k - n_1^k, \qquad i = 2, \dots, N. \quad (21)$$

We assume that ξ_w and n_i^k are independent. We collect all the measurements when an estimate of the clock skew is available as follows:

$$\bar{\mathbf{z}} = \left[\bar{\mathbf{z}}_1^T \cdots \bar{\mathbf{z}}_K^T\right]^T \in \mathbb{R}^{K(N-1)}, \quad (22)$$

where

$$\bar{\mathbf{z}}_k = \left[\bar{z}_{2,1}^k \ \ldots \ \bar{z}_{N,1}^k\right]^T \in \mathbb{R}^{(N-1)}. \tag{23}$$

Considering that the vector $\bar{\mathbf{z}}$ is a Gaussian random vector $\bar{\mathbf{z}} \sim \mathcal{N}(\bar{\boldsymbol{\mu}}_K, \bar{\mathbf{C}}_K)$ with

$$\begin{aligned}\bar{\boldsymbol{\mu}}_K &= \mathbf{1}_K \otimes \hat{w}\left[d_{2,1}\ldots d_{N,1}\right]^T,\\ \bar{\mathbf{C}}_K &= \text{blkdiag}\Big(\underbrace{\bar{\mathbf{C}},\ldots,\bar{\mathbf{C}}}_{K\text{times}}\Big),\end{aligned} \tag{24}$$

and

$$\begin{aligned}\bar{\mathbf{C}} =& \text{diag}(\sigma_2^2,\ldots,\sigma_N^2) + \sigma_1^2 \mathbf{1}_{N-1}\mathbf{1}_{N-1}^T\\ &+ \sigma_w^2\left[d_{2,1}\ \ldots\ d_{N,1}\right]^T\left[d_{2,1}\ \ldots\ d_{N,1}\right],\end{aligned} \tag{25}$$

the entries of the Fisher information matrix is obtained as [23, Ch. 3]

$$\begin{aligned}\bar{J}_{nm} = [\bar{\mathbf{J}}]_{nm} =& \left[\frac{\partial \bar{\boldsymbol{\mu}}_K}{\partial x_n}\right]^T \bar{\mathbf{C}}_K^{-1}\left[\frac{\partial \bar{\boldsymbol{\mu}}_K}{\partial x_m}\right]\\ &+\frac{1}{2}\text{tr}\left(\bar{\mathbf{C}}_K^{-1}\frac{\partial \bar{\mathbf{C}}_K}{\partial x_m}\bar{\mathbf{C}}_K^{-1}\frac{\partial \bar{\mathbf{C}}_K}{\partial x_n}\right),\\ & n=1,2,\ m=1,2.\end{aligned} \tag{26}$$

Then, the CRLB for the position estimate is given by

$$\mathbb{E}\{\|\hat{\mathbf{x}}-\mathbf{x}\|^2\} \geq \frac{\bar{J}_{11}+\bar{J}_{22}}{\bar{J}_{11}\bar{J}_{22}-\bar{J}_{12}^2}\cdot \tag{27}$$

This CRLB expression will be useful for providing theoretical limits on the performance of position estimators that are based on already available estimates of the clock skew parameter. In addition, for $\sigma_w = 0$ (i.e., no estimation errors), the CRLB expression covers the special case in which the clock skew parameter is perfectly known.

IV. Suboptimal Estimators

To solve the MLE formulated in (12) using an iterative algorithm, we need a suitable initial point that is sufficiently close to the optimal solution. In this section, we propose two suboptimal estimators that provide such initial points. In particular, we consider a two step estimation procedure: coarse and fine. For the coarse estimation step, we derive two suboptimal estimators based on semidefinite programming (SDP) relaxation and linear least squares (LLS). In the fine estimation step, we derive a linear model and employ a technique based on the regularized least squares critrerion.

A. Coarse estimate

We first express the clock skew parameter as $w = 1+\delta$, where δ is a small value.[4] Dividing both sides of (3) by w and using the approximation $1/(1+\delta) \simeq 1-\delta$, we can approximate the RDOA measurement in (4) as

$$\begin{aligned}&z_{i,1}^k(1-\delta) \simeq d_{i,1} + (1-\delta)(n_i^k - n_1^k),\\ &i=2,\ldots,N,\ k=1,\ldots,K,\end{aligned} \tag{28}$$

[4]This is a reasonable model since the deviation of the clock skew parameter from the ideal value of $w=1$ is not significant for most practical clocks.

which can be further simplified (for the purpose of obtaining the approximate MLE in Section IV-A1 in which the covariance matrix is independent of the unknown parameter δ) as

$$\begin{aligned}&z_{i,1}^k(1-\delta) \simeq d_{i,1} + (n_i^k - n_1^k),\\ &i=2,\ldots,N,\ k=1,\ldots,K.\end{aligned} \tag{29}$$

It is noted that keeping δ in (28) for the SDP formulation in the next section complicates the problem. In fact the covariance matrix of measurement noise will be dependent on the unknown parameter δ and therefore it is difficult to convert the corresponding MLE to an SDP problem. However, for the LLS formulation we apply a nonlinear processing on measurements in (28) that makes the measurement noise be dependent on both δ and unknown distance. Hence, neglecting δ does not change the complexity of the problem considerably. As explained later, in the LLS approach, we first neglect the effect of the unknown parameters on the covariance matrix of the measurement noise and find a first estimate of the unknown parameters. We then use the first estimate to approximate the covariance matrix.

1) Semidefinite Programming: In this section, we first apply the maximum likelihood criterion to the model in (29) and then change it to an SDP problem. The MLE for the model in (29) can be obtained as

$$\begin{aligned}&[\hat{\mathbf{x}}^T\ \hat{\delta}] =\\ &\underset{[\mathbf{x}^T\ \delta]\in\mathbb{R}^3}{\arg\min}\sum_{k=1}^K\left(\mathbf{z}_k(1-\delta)-\mathbf{P}\mathbf{d}\right)^T\mathbf{C}^{-1}\left(\mathbf{z}_k(1-\delta)-\mathbf{P}\mathbf{d}\right),\end{aligned} \tag{30}$$

where $\mathbf{z}_k$ is as in (6) and matrix $\mathbf{P}$ and vector $\mathbf{d}$ are given by

$$\mathbf{P} = \begin{bmatrix} -1 & 1 & 0 & 0 & \ldots & 0\\ -1 & 0 & 1 & 0 & \ldots & 0\\ \vdots & \vdots & \vdots & \vdots & \vdots & \vdots\\ -1 & 0 & 0 & 0 & \ldots & 1\end{bmatrix}, \tag{31a}$$

$$\mathbf{d} = [d(\mathbf{a}_1,\mathbf{x})\ d(\mathbf{a}_2,\mathbf{x})\ \ldots\ d(\mathbf{a}_N,\mathbf{x})]^T. \tag{31b}$$

To solve (30), we use an alternative projection approach. That is, we first optimize the MLE objective function with respect to the unknown parameter δ. Taking the derivative of the objective function in (30) with respect to δ and equating to zero yield the following expression for δ:

$$\delta = 1 - \mathbf{g}^T\mathbf{d}\ , \tag{32}$$

where

$$\mathbf{g} = \frac{\sum_{k=1}^K \mathbf{P}^T\mathbf{z}_k\mathbf{C}^{-1}}{\sum_{k=1}^K \mathbf{z}_k^T\mathbf{C}^{-1}\mathbf{z}_k}. \tag{33}$$

In the next step of the alternative projection approach, we insert the expression in (32) into the MLE cost function in (30). We also note that δ is small and then impose a constraint (an upper bound) on its absolute value, i.e, $|\delta| \leq \delta_{\max}$, where $\delta_{\max}$ is a reasonable upper bound on δ. After some manipulation, we can express the MLE for the position as

$$\begin{aligned}&\underset{\mathbf{x}\in\mathbb{R}^2}{\text{minimize}}\ \mathbf{d}^T\mathbf{Q}\mathbf{d}\\ &\text{subject to } |1-\mathbf{g}^T\mathbf{d}| \leq \delta_{\max}\end{aligned} \tag{34}$$

where $\mathbf{Q}$ is given by

$$\mathbf{Q} = \sum_{k=1}^{K} \left(\mathbf{z}_k \frac{\sum_{k=1}^{K} \mathbf{z}_k^T \mathbf{C}^{-1} \mathbf{P}}{\sum_{k=1}^{K} \mathbf{z}_k^T \mathbf{C}^{-1} \mathbf{z}_k} - \mathbf{P} \right)^T \mathbf{C}^{-1} \left(\mathbf{z}_k \frac{\sum_{k=1}^{K} \mathbf{z}_k^T \mathbf{C}^{-1} \mathbf{P}}{\sum_{k=1}^{K} \mathbf{z}_k^T \mathbf{C}^{-1} \mathbf{z}_k} - \mathbf{P} \right). \quad (35)$$

The optimization problem in (34) is nonconvex and difficult to solve. In order to obtain a convex problem, we express $\mathbf{d}^T\mathbf{Q}\mathbf{d}$ as $\mathbf{d}^T\mathbf{Q}\mathbf{d} = \operatorname{tr}(\mathbf{Q}\mathbf{V})$, where $\mathbf{V} = \mathbf{d}\mathbf{d}^T$, and relax the nonconvex constraint $\mathbf{V} = \mathbf{d}\mathbf{d}^T$ as follows. Recalling that $v_{ij} = [\mathbf{V}]_{ij} = \|\mathbf{a}_i - \mathbf{x}\|\|\mathbf{a}_j - \mathbf{x}\|$, we can represent the diagonal entries of $\mathbf{V}$ as

$$v_{ii} = \|\mathbf{a}_i - \mathbf{x}\|^2 = \operatorname{tr}\left(\begin{bmatrix} \mathbf{I}_2 & -\mathbf{a}_i \\ -\mathbf{a}_i^T & \|\mathbf{a}_i\|^2 \end{bmatrix} \mathbf{Z} \right), \quad (36)$$

where $\mathbf{Z} = \begin{bmatrix} \mathbf{x}^T & 1 \end{bmatrix}^T \begin{bmatrix} \mathbf{x}^T & 1 \end{bmatrix}$, i.e., $\mathbf{Z}$ is a rank-1 positive semidifinite matrix. In addition, using Cauchy-Schwarz inequality, we can express $v_{ij}, i \neq j$ as

$$v_{ij} = \|\mathbf{a}_i - \mathbf{x}\|\|\mathbf{a}_j - \mathbf{x}\| \geq \left| \operatorname{tr}\left(\begin{bmatrix} \mathbf{I}_2 & -\mathbf{a}_i \\ -\mathbf{a}_j^T & \mathbf{a}_i^T\mathbf{a}_j \end{bmatrix} \mathbf{Z} \right) \right|. \quad (37)$$

Hence, the problem in (34) can be written as:

$$\begin{aligned} &\underset{\mathbf{z}\in\mathbb{S}^3;\mathbf{d}\in\mathbb{R}_+^N;\mathbf{V}\in\mathbb{S}^N}{\text{minimize}} \quad \mathbf{d}^T\mathbf{Q}\mathbf{d} \\ &\text{subject to } \operatorname{tr}\left(\begin{bmatrix} \mathbf{I}_2 & -\mathbf{a}_i \\ -\mathbf{a}_j^T & \mathbf{a}_i^T\mathbf{a}_j \end{bmatrix} \mathbf{Z} \right) \leq v_{ij}, \quad i \neq j, \\ &\operatorname{tr}\left(\begin{bmatrix} -\mathbf{I}_2 & \mathbf{a}_i \\ \mathbf{a}_j^T & -\mathbf{a}_i^T\mathbf{a}_j \end{bmatrix} \mathbf{Z} \right) \leq v_{ij}, \quad i \neq j, \\ &\operatorname{tr}\left(\begin{bmatrix} \mathbf{I}_2 & -\mathbf{a}_i \\ -\mathbf{a}_i^T & \|\mathbf{a}_i\|^2 \end{bmatrix} \mathbf{Z} \right) = v_{ii}, \\ &\mathbf{g}^T\mathbf{d} \leq 1 + \delta_{\text{max}}, \\ &-\mathbf{g}^T\mathbf{d} \leq \delta_{\text{max}} - 1, \\ &\mathbf{V} = \mathbf{d}\mathbf{d}^T, \quad \mathbf{Z} \succeq 0, \quad \operatorname{rank}(\mathbf{Z}) = 1, \\ &[\mathbf{Z}]_{3,3} = 1, \quad i, j = 1, \ldots, N. \end{aligned} \quad (38)$$

The nonconvex problem in (38) can be changed to a convex problem by dropping the rank-1 constraint $\operatorname{rank}(\mathbf{Z}) = 1$ and relaxing the nonconvex constraint $\mathbf{V} = \mathbf{d}\mathbf{d}^T$ to a convex one, i.e., $\mathbf{V} \succeq \mathbf{d}\mathbf{d}^T$. Then, the convex optimization problem, called SDP, can be cast as

$$\begin{aligned} &\underset{\mathbf{z}\in\mathbb{S}^3;\mathbf{d}\in\mathbb{R}_+^N;\mathbf{V}\in\mathbb{S}^N}{\text{minimize}} \quad \mathbf{d}^T\mathbf{Q}\mathbf{d} \\ &\text{subject to } \operatorname{tr}\left(\begin{bmatrix} \mathbf{I}_2 & -\mathbf{a}_i \\ -\mathbf{a}_j^T & \mathbf{a}_i^T\mathbf{a}_j \end{bmatrix} \mathbf{Z} \right) \leq v_{ij}, \quad i \neq j, \\ &\operatorname{tr}\left(\begin{bmatrix} -\mathbf{I}_2 & \mathbf{a}_i \\ \mathbf{a}_j^T & -\mathbf{a}_i^T\mathbf{a}_j \end{bmatrix} \mathbf{Z} \right) \leq v_{ij}, \quad i \neq j, \\ &\operatorname{tr}\left(\begin{bmatrix} \mathbf{I}_2 & -\mathbf{a}_i \\ -\mathbf{a}_i^T & \|\mathbf{a}_i\|^2 \end{bmatrix} \mathbf{Z} \right) = v_{ii}, \\ &\mathbf{g}^T\mathbf{d} \leq 1 + \delta_{\text{max}}, \\ &-\mathbf{g}^T\mathbf{d} \leq \delta_{\text{max}} - 1, \\ &\begin{bmatrix} \mathbf{V} & \mathbf{d} \\ \mathbf{d}^T & 1 \end{bmatrix} \succeq 0, \quad \mathbf{Z} \succeq 0, \\ &[\mathbf{Z}]_{3,3} = 1, \quad i, j = 1, \ldots, N. \end{aligned} \quad (39)$$

Note that the constraint $\mathbf{V} \succeq \mathbf{d}\mathbf{d}^T$ is expressed as a linear matrix inequality using the Schur complement [25]. If the optimal solution of (39), i.e., $\hat{\mathbf{Z}}$, has rank-1 property and $\mathbf{V} = \mathbf{d}\mathbf{d}^T$, then the optimal solution is at hand. Otherwise, we can apply a rank-1 approximation technique to improve the position estimate [26].

2) Linear least squares (LLS): In this section, we derive a linear estimator to estimate the position of the target node based on a nonlinear processing technique. We first translate the network such that the first reference node lies at the origin. In particular, we define $\mathbf{a}'_i = \mathbf{a}_i - \mathbf{a}_1$ for $i = 1, \ldots, N$ and $\mathbf{t} = \mathbf{x} - \mathbf{a}_1$. Then, we move $d(\mathbf{a}_1, \mathbf{x})$ in (28) (remembering that $d_{i,1} = d(\mathbf{a}_i, \mathbf{x}) - d(\mathbf{a}_1, \mathbf{x})$) to the right-hand-side in the translated coordinates as

$$z_{i,1}^k (1 - \delta) + \|\mathbf{t}\| \simeq d(\mathbf{a}'_i, \mathbf{t}) + (1 - \delta)(n_i^k - n_1^k), \quad i = 2, \ldots, N. \quad (40)$$

Assume that the noise is small compared to the distance $d(\mathbf{a}'_i, \mathbf{t})$. Then, squaring both sides of (40) and dropping the small term, we get

$$\begin{aligned} &(z_{i,1}^k)^2(1-\delta)^2 + 2z_{i,1}^k(1-\delta)\|\mathbf{t}\| + \|\mathbf{t}\|^2 \simeq \\ &\|\mathbf{a}'_i\|^2 - 2(\mathbf{a}'_i)^T\mathbf{t} + \|\mathbf{t}\|^2 + 2d(\mathbf{a}'_i, \mathbf{t})(1-\delta)(n_i^k - n_1^k), \\ &i = 2, \ldots, N. \end{aligned} \quad (41)$$

Assuming small δ, we can write $(1 - \delta)^2 \simeq 1 - 2\delta$. Hence, we obtain a linear model based on unknown vector $\boldsymbol{\theta} = [\mathbf{t}^T \ \|\mathbf{t}\| \ \delta]^T$ as

$$\bar{z}_i^k = (\mathbf{g}_i^k)^T\boldsymbol{\theta} + \xi_i^k, \quad (42)$$

where $\mathbf{g}_i^k = 2[-(\mathbf{a}'_i)^T \ -z_{i,1}^k \ (z_{i,1}^k)^2]^T$, $\bar{z}_i^k = (z_{i,1}^k)^2 - \|\mathbf{a}'_i\|^2$ and $\xi_i^k = 2d(\mathbf{a}'_i, \mathbf{t})(1-\delta)(n_i^k - n_1^k) + 2\delta\|\mathbf{t}\|z_{i,1}^k$. Following the procedure explained above for all measurements, we obtain a linear model in the matrix form as

$$\mathbf{h} = \mathbf{G}\boldsymbol{\theta} + \boldsymbol{\xi}, \quad (43)$$

where matrix $\mathbf{G}$, and vectors $\mathbf{h}$ and $\boldsymbol{\xi}$ are computed as

$$\begin{aligned} \mathbf{G} &= \begin{bmatrix} \mathbf{g}_2^1 & \ldots & \mathbf{g}_1^K & \ldots & \mathbf{g}_1^K & \ldots & \mathbf{g}_N^K \end{bmatrix}^T \in \mathbb{R}^{(N-1)K\times 3}, \\ \mathbf{h} &= [\bar{z}_2^1 \ \ldots \ \bar{z}_N^1 \ \ldots \ \bar{z}_2^K \ \ldots \ \bar{z}_N^K]^T \in \mathbb{R}^{(N-1)K}, \\ \boldsymbol{\xi} &= [\xi_2^1 \ \ldots \ \xi_N^1 \ \ldots \ \xi_2^K \ \ldots \ \xi_N^K]^T \in \mathbb{R}^{(N-1)K}. \end{aligned} \quad (44)$$

Note that the noise vector $\boldsymbol{\xi}$ is a random vector with a nonzero mean. In fact, $\mathbb{E}(\boldsymbol{\xi}) = 2\delta\|\mathbf{t}\|\boldsymbol{\mu}_K$, where $\boldsymbol{\mu}_K$ is given in (8). The covariance matrix of $\boldsymbol{\xi}$ can be computed as

$$\mathbf{C}_{\boldsymbol{\xi}} = \operatorname{blkdiag}\Big(\underbrace{\mathbf{D}, \ldots, \mathbf{D}}_{K \text{ times}}\Big)\mathbf{C}_K \operatorname{blkdiag}\Big(\underbrace{\mathbf{D}, \ldots, \mathbf{D}}_{K \text{ times}}\Big), \quad (45)$$

where

$$\begin{aligned} \mathbf{D} = 4\operatorname{diag}\big(&d(\mathbf{a}'_2, \mathbf{t})(1-\delta) + \delta\|\mathbf{t}\|, \ldots, d(\mathbf{a}'_N, \mathbf{t})(1-\delta) \\ &+ \delta\|\mathbf{t}\|\big). \end{aligned} \quad (46)$$

Using the least squares criterion, a solution to (43) is obtained as [23]

$$\hat{\boldsymbol{\theta}} = (\mathbf{G}^T\mathbf{C}_{\boldsymbol{\xi}}^{-1}\mathbf{G})^{-1}\mathbf{G}^T\mathbf{C}_{\boldsymbol{\xi}}^{-1}(\mathbf{h} - \mathbb{E}(\boldsymbol{\xi})). \quad (47)$$

Note that the mean vector $\mathbb{E}(\boldsymbol{\xi})$ and the inverse of the covariance matrix $\mathbf{C}_{\boldsymbol{\xi}}^{-1}$ are unknown in advance since they are dependent on the unknown parameters. We first assign a zero vector and an identity matrix to the mean vector and the covariance matrix, respectively, and find an estimate of the unknown parameters. Then, we approximate the mean vector and the covariance matrix and recalculate the estimate given in (47).

The covariance matrix of the estimate in (47) is given by [23]

$$\mathbf{C}_{\hat{\boldsymbol{\theta}}} = (\mathbf{G}^T \mathbf{C}_{\boldsymbol{\xi}}^{-1} \mathbf{G})^{-1}. \tag{48}$$

Remark 1: In cases that the observation matrix $\mathbf{G}$ is ill-conditioned, we can use a regularization technique in (47) to obtain a solution to the linear model in (43). When the regularization parameter applies to the last component of the unknown vector $\boldsymbol{\theta}$, it has a nice interpretation. That is, the deviation of the clock skew from the ideal clock is extremely small.

Remark 2: The procedure for approximating the covariance matrix and mean vector of $\boldsymbol{\xi}$ can be iterated for several times. However, in practice one round of updating is enough to achieve good performance.

We can further improve the accuracy of the estimate in (47) by taking the relation between the elements of the estimate vector $\hat{\boldsymbol{\theta}}$ into account. Each element of (47) can be written as

$$\begin{aligned} [\hat{\boldsymbol{\theta}}]_1 &= t_1 + \chi_1, \\ [\hat{\boldsymbol{\theta}}]_2 &= t_2 + \chi_2, \\ [\hat{\boldsymbol{\theta}}]_3 &= \|\mathbf{t}\| + \chi_3, \end{aligned} \tag{49}$$

where $\boldsymbol{\chi} = [\chi_1 \ \chi_2 \ \chi_3]^T$ denotes the estimation error, i.e., $\boldsymbol{\chi} = \hat{\boldsymbol{\theta}} - \boldsymbol{\theta}$, and $\mathbf{t} = [t_1 \ t_2]^T$. Suppose that the estimation errors are considerably small. Therefore, squaring both sides of the elements in (49) yields

$$\begin{aligned} [\hat{\boldsymbol{\theta}}]_1^2 &\simeq t_1^2 + 2t_1\chi_1, \\ [\hat{\boldsymbol{\theta}}]_2^2 &\simeq t_2^2 + 2t_2\chi_2, \\ [\hat{\boldsymbol{\theta}}]_3^2 &\simeq \|\mathbf{t}\|^2 + 2\|\mathbf{t}\|\chi_3. \end{aligned} \tag{50}$$

Hence, the relation between the estimated elements in (47) can be obtained using (50) as

$$\mathbf{u} = \mathbf{B}\boldsymbol{\phi} + \boldsymbol{\nu}, \tag{51}$$

where

$$\begin{aligned} \boldsymbol{\nu} &= [2t_1\chi_1 \ 2t_2\chi_2 \ 2\|\mathbf{t}\|\chi_3]^T, \\ \mathbf{u} &= \left[[\hat{\boldsymbol{\theta}}]_1^2 \ [\hat{\boldsymbol{\theta}}]_2^2 \ [\hat{\boldsymbol{\theta}}]_3^2\right]^T, \\ \boldsymbol{\phi} &= \left[t_1^2 \ t_2^2\right]^T, \\ \mathbf{B} &= \begin{bmatrix} 1 & 0 \\ 0 & 1 \\ 1 & 1 \end{bmatrix}. \end{aligned} \tag{52}$$

Then, the least squares solution to (51) is obtained as

$$\hat{\boldsymbol{\phi}} = (\mathbf{B}^T \mathbf{C}_{\boldsymbol{\nu}}^{-1} \mathbf{B})^{-1} \mathbf{C}_{\boldsymbol{\nu}}^{-1} \mathbf{B}^T \mathbf{u}, \tag{53}$$

where the covariance matrix of $\mathbf{C}_{\boldsymbol{\nu}}$ can be computed as

$$\mathbf{C}_{\boldsymbol{\nu}} = \mathrm{diag}(t_1, t_2, \|\mathbf{t}\|) \left[\mathbf{C}_{\hat{\boldsymbol{\theta}}}\right]_{1:3,1:3} \mathrm{diag}(t_1, t_2, \|\mathbf{t}\|). \tag{54}$$

To compute the covariance matrix $\mathbf{C}_{\boldsymbol{\nu}}$, we use the estimate given in (47) instead of the true values of t_1, t_2, and $\|\mathbf{t}\|$, which are unknown *a-priori*.

Based on the preceding calculations, the target position can be obtained as follows:

$$\tilde{x}_j = \mathrm{sgn}([\boldsymbol{\theta}]_j)\sqrt{\left|[\hat{\boldsymbol{\phi}}]_j\right|} + a_{1,j} \ , \quad j = 1, 2 \,, \tag{55}$$

where the signum function $\mathrm{sgn}(x)$ is defined as

$$\mathrm{sgn}(x) = \begin{cases} 1 & \text{if } x \geq 0, \\ -1 & \text{if } x < 0. \end{cases} \tag{56}$$

Note that using a similar approach as employed in [19], [27], we can compute the covariance of the estimate in (55).

B. Fine estimate

The approaches considered in the coarse estimation step provide good initial points for further refining the position estimates. One method is to implement the MLE using an iterative search approach initialized with the estimate in the coarse estimation step. In this section, we propose another approach with lower complexity. To that end, we first update the estimate of the clock skew. Assuming an estimate of the location $\bar{\mathbf{x}}$ ($\bar{\mathbf{x}} = \hat{\mathbf{x}}$ for $\hat{\mathbf{x}}$ given by the SDP solution in (39) or $\bar{\mathbf{x}} = \tilde{\mathbf{x}}$ for $\tilde{\mathbf{x}}$ provided by the LLS in (55)), an estimate of the clock skew can be obtained from (4) using the method of moments [23] as

$$\hat{w} = \frac{\sum_{k=1}^K \sum_{i=2}^N z_{i,1}^k}{K \sum_{i=2}^N \bar{d}_{i,1}}, \tag{57}$$

where $\bar{d}_{i,1} = \bar{d}_i - \bar{d}_1$ and $\bar{d}_i = \|\bar{x} - \mathbf{a}_i\|$. Now considering an estimate of the clock skew in (57) and applying the first order Taylor series expansion about $\bar{\mathbf{x}}$ to (4), we get the following expression:

$$z_{i,1}^k \simeq \hat{w}\bar{d}_{i,1} + \bar{\mathbf{g}}_i^T \Delta\mathbf{x} + n_i^k - n_1^k, \tag{58}$$

where $\bar{\mathbf{g}}_i = \hat{w}(\bar{\mathbf{x}} - \mathbf{a}_i)/\bar{d}_i - \hat{w}(\bar{\mathbf{x}} - \mathbf{a}_1)/\bar{d}_1$, and $\Delta\mathbf{x} = \mathbf{x} - \bar{\mathbf{x}}$. Thus, we arrive at the following linear model to estimate the estimation error $\Delta\mathbf{x}$:

$$\bar{\mathbf{t}} = \bar{\mathbf{G}}\Delta\mathbf{x} + \boldsymbol{\vartheta}, \tag{59}$$

where

$$\begin{aligned} \boldsymbol{\vartheta} &= [n_2^1 - n_1^1 \ \ldots \ n_N^1 - n_1^1 \ldots n_2^K - n_1^K \ldots n_N^K - n_1^K]^T \\ \bar{\mathbf{t}} &= [z_{2,1}^1 - \hat{w}\bar{d}_{2,1} \ \ldots \ z_{N,1}^1 - \hat{w}\bar{d}_{N,1} \ \ldots \ z_{2,1}^K - \hat{w}\bar{d}_{2,1} \\ &\quad \ldots \ z_{N,1}^K - \hat{w}\bar{d}_{N,1}]^T, \\ \mathbf{G} &= \mathbf{I}_K \otimes [\bar{\mathbf{g}}_2^T \ \ldots \ \bar{\mathbf{g}}_N^T]^T. \end{aligned} \tag{60}$$

The assumption in deriving the model in (59) requires that the estimation error $\Delta\mathbf{x}$, be small enough. We take this assumption into account and apply a regularized least squares (Tikhonov regularization technique) to find an estimate of $\Delta\mathbf{x}$ as [19], [28], [29]

$$\hat{\Delta}\mathbf{x} = (\bar{\mathbf{G}}^T \mathbf{C}_K^{-1} \bar{\mathbf{G}} + \lambda \mathbf{I}_2)^{-1} \bar{\mathbf{G}}^T \mathbf{C}_K^{-1} \bar{\mathbf{t}}, \tag{61}$$

where λ defines a trade-off between $\|\Delta\mathbf{x}\|^2$ and $(\bar{\mathbf{G}}\Delta\mathbf{x} - \bar{\mathbf{t}})^T \mathbf{C}_K^{-1} (\bar{\mathbf{G}}\Delta\mathbf{x} - \bar{\mathbf{t}})$.

Finally, the updated estimate is obtained as

$$\hat{\bar{\mathbf{x}}} = \bar{\mathbf{x}} + \hat{\Delta}\mathbf{x}. \tag{62}$$

C. Complexity analysis

In this section we evaluate the complexity of the estimators considered in this study based on the total number of the floating-point operations or *flops*. We assume that an addition, subtraction, and multiplicationin in opertion in the real domain can be computed by one flop [28], and that a division or square root operation needs r flops (usually 20 to 30 flops [30]). We calculate the total number of flops for every method and express it as a polynomial of the free parameters. Then, we compute the complexity as the order of growth for each approach. To simplify the results, we keep only the leading terms of the complexity expressions.

1) The maximum likelihood estimator: As previously mentioned, the MLE is nonlinear and nonconvex. Therefore the complexity of the MLE highly depends on the solution method. In addition, the complexity of each method also depends on a number of parameters, e.g., the number of iterations, the initial point, and the solution accuracy. Here we compute the cost of evaluating the objective function of the MLE in (12) for a certain point and also the cost of the Gauss-Newton (GN) approach to solve the MLE when a good initial point is available. We note that we need $(r+5)$ flops to compute a distance. The number of flops required to evaluate the objective function of the MLE is approximately given by $K(N-1)(2N+2+r)+N(6+r)$. Then, considering the leading term, the complexity of evaluating the MLE objective function is expressed as $O(KN^2)$. It can be shown that the complexity of every Newton step is on the order of $(KN)^3$. Then the total cost of the GN approach for solving the MLE is $O(I_{\mathrm{GN}}(KN)^3)$, where I_{GN} is the number of iterations in the GN method to converge to the solution.

2) The semidefinite programming: The worst-case complexity of the SDP in (39) is given by $O(I_{SDP}(\sum_i^{N_c}(L^2s_i^2+Ls_i^3)+L^3)\log(1/\epsilon))$ [31], where L is the number of equality constraints, s_i is the dimension of the ith semidefinite cone, N_c is the number of semidefinite constraints, I_{SDP} is the number of iterations, and ϵ is the accuracy of the SDP solution. Therefore, the complexity of the SDP formulated in (39) is given as

$$\text{SDP cost} \simeq O\Bigg(I_{\mathrm{SDP}}\Big((N+1)^2\big((N+1)^3+3^3 + (N+1)^3+9(N+1)\big)+(N+1)^3\Big)\log(1/\epsilon)\Bigg). \quad (63)$$

Then, the number of iterations I_{SDP} is approximated as $I_{\mathrm{SDP}} \simeq O(N^{1/2})$ [31].

3) The linear least squares: To compute the complexity of the LLS, we note that the matrix $\mathbf{C}_{\boldsymbol{\xi}}$ is a block diagonal matrix. In addition, since the matrix $\mathbf{C}_K$ in (8) is fixed and diagonal, the inverse of $\mathbf{C}_K$ can be computed once and used later. Then the complexity of the linear estimator in (47) can be computed as

$$\begin{aligned}&\text{Flops of LLS in (47)}\\ &\simeq \underbrace{(N-1)(3K+r+10)+r+5}_{\text{cost of computing } \mathbf{h}-\mathbb{E}(\boldsymbol{\xi})}\\ &+\underbrace{(N-1)(r+7)+r+5}_{\text{cost of computing } \mathbf{D}}++\underbrace{(N-1)^2(r+1)}_{\text{cost of computing } \mathbf{C}_{\boldsymbol{\xi}}^{-1}}\\ &+\underbrace{6K(N-1)}_{\text{cost of } \mathbf{G}^T\mathbf{C}_{\boldsymbol{\xi}}^{-1}}+\underbrace{6K(N-1)}_{\text{cost of } \mathbf{G}^T\mathbf{C}_{\boldsymbol{\xi}}^{-1}\mathbf{G}}+\underbrace{3K(N-1)}_{\text{cost of } \mathbf{C}_{\boldsymbol{\xi}}^{-1}\mathbf{G}(\mathbf{h}-\mathbb{E}(\boldsymbol{\xi}))}\\ &+\underbrace{33.}_{\text{cost of } (\mathbf{G}^T\mathbf{C}_{\boldsymbol{\xi}}^{-1}\mathbf{G})^{-1}\mathbf{G}^T\mathbf{C}_{\boldsymbol{\xi}}^{-1}(\mathbf{h}-\mathbb{E}(\boldsymbol{\xi}))}\end{aligned} \quad (64)$$

It can easily be verified that the complexity of the correction technique compared to the LLS in (47) is negligible. Then, the complexity of the the linear estimator (for large K and N) can be computed as $O(18KN+rN^2)$.

4) Fine estimation step: In a similar way the complexity of the fine estimation step can be computed as

$$\begin{aligned}\text{Finestep} \simeq\ &\underbrace{N(5+r)}_{\text{cost of computing } \bar{d}_i}+\underbrace{N(K+1)+r-K}_{\text{cost of computing } \hat{w}}\\ &+\underbrace{(K+1)(N-1)}_{\text{cost of computing } \bar{\mathbf{t}}}+\underbrace{2(KN)^2+2N(r+2)-2}_{\text{cost of computing } \bar{\mathbf{G}}^T\mathbf{C}_K^{-1}}\\ &+\underbrace{2KN+1+8}_{\text{cost of } (\bar{\mathbf{G}}^T\mathbf{C}_K^{-1}\bar{\mathbf{G}}+\lambda\mathbf{I}_2)^{-1}}+\underbrace{2KN}_{\text{cost of } \bar{\mathbf{G}}^T\mathbf{C}_K^{-1}\bar{\mathbf{t}}}\\ &+\underbrace{6.}_{\text{cost of } (\bar{\mathbf{G}}^T\mathbf{C}_K^{-1}\bar{\mathbf{G}}+\lambda\mathbf{I}_2)^{-1}\bar{\mathbf{G}}^T\mathbf{C}_K^{-1}\bar{\mathbf{t}}}\end{aligned} \quad (65)$$

Then the complexity of the fine estimation step can be approximated as $O(2K^2N^2)$.

Table I summarizes the complexity of the different approaches for large K and N. Note that for small K and N, the cost for different approaches can be different from the ones in Table I.

We have also measured the average running time of different algorithms for a network consisting of 8 reference nodes as considered in Section V. The algorithms have been implemented in Matlab 2012 on a MacBook Pro (Processor 2.3 GHz Intel Core i7, Memory 8 GB 1600 MHz DDR3). To implement the MLE, we use the Matlab function named *lsqnonlin* [32] initialized with the true values of the location and the clock skew. To implement the SDP, we use the *CVX* toolbox [33]. We run the algorithms for 200 realizations of the network and compute the average running time in ms as shown in Table II. It is noted that although the MLE has lower complexity than the SDP, we need a good initial point for the GN algorithm, which in turn poses further complexity. From Table I and Table II, it is observed that the proposed approaches have reasonable complexity, especially the linear estimator.

V. Simulation Results

A. Simulation Setup

Computer simulations are conducted in order to evaluate the performance of the proposed approaches. Fig. 3 illustrates the

TABLE I
COMPLEXITY OF DIFFERENT APPROACHES.

Method	Complexity
Evaluation of the MLE objective function at a point	$O(KN^2)$
MLE using GN (true initialization)	$O(I_{\mathrm{GN}}(KN)^3)$
SDP	$O(I_{\mathrm{SDP}}(N+1)^5)\log(1/\epsilon)),\ I_{\mathrm{SDP}} \simeq O(N^{1/2})$
LLS	$O(18KN + rN^2)$
Fine estimation step	$O(2K^2N^2)$

TABLE II
AVERAGE RUNNING TIME OF DIFFERENT APPROACHES.

Method	Time (ms)
MLE using (true initialization)	247
SDP	525
LLS	1
Fine estimation step	0.9

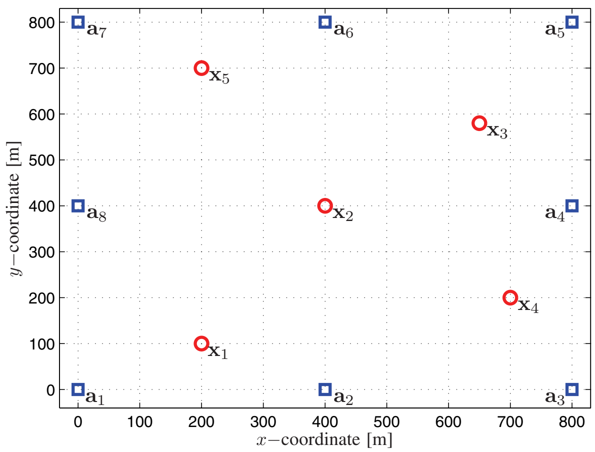

Fig. 3. A 2-D network deployment used in the simulations (blue squares and red circles show reference and target nodes, respectively).

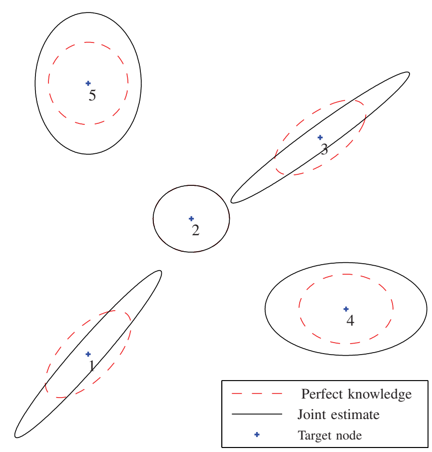

Fig. 5. Ellipsis uncertainty region (for $K = 3$) for $\sigma = 10$ [m].

positions of the reference and target nodes for a 2-D network. In the simulations, the clock skew is randomly drawn from $[0.995, 1.005]$, and it is assumed that the standard deviation of the noise is the same for all nodes, i.e., $\sigma_i = \sigma, \forall i$. In the simulations, we assume that a reference node sends its $(k+1)$th signal after other reference nodes complete transmitting the kth signal. For simplicity of implementation, we consider the order of TDOA measurements according to (5) and (6). To evaluate the performance of different approaches, we consider the root-mean-squared error (RMSE) and the cumulative distribution function (CDF) of the position error.

B. CRLB Analysis

In this section, we investigate CRLBs on position estimation in the presence and absence of clock skew information. Fig. 4 shows the CRLBs for various target nodes and for different values of K. We compare the CRLBs in two scenarios: i) joint estimation of the position and the clock skew parameter (i.e., unknown clock skew), and ii) perfect knowledge of the clock skew parameter (i.e., perfectly synchronized clocks). It is observed that for small values of σ, the CRLBs are close to each other in both scenarios and the degradation due to the unknown clock skew increases with the standard deviation of the noise, σ. Except for target node two located at the center of the reference nodes, adding a new unknown variable as a nuisance parameter (i.e., the clock skew parameter) deteriorates the accuracy of position estimates.

To visualize the effects of an unknown clock skew on the position estimation accuracy, we plot the CRLB as an ellipsoid uncertainty in Fig. 5 for $\sigma = 10$ m. We scale the coordinates of the target nodes so that the difference between the two scenarios is clearly visible. We observe from the figure that different locations for the target nodes show different behaviors. For target node two, two ellipsoids coincide while for the other target nodes the volume of the ellipsoid for the unknown clock skew parameter scenario is larger than the one for the perfect synchronization scenario.

In the next simulations, we compare the performance of the joint position and clock skew estimation with the position estimation when an estimate of the clock skew is available. As mentioned in Section III-B, we model the available clock skew estimate as a Gaussian random variable, that is, $\hat{w} \sim \mathcal{N}(w, \sigma_w^2)$. The CRLBs for the two cases are plotted in Fig. 6 for target one when $K = 3$. It is observed from the figure that when the standard deviation of the clock skew estimate increases, the joint estimation technique outperforms the one that is based on available estimates of the clock skew. It is also seen for low SNRs (high σ's) that the joint estimation

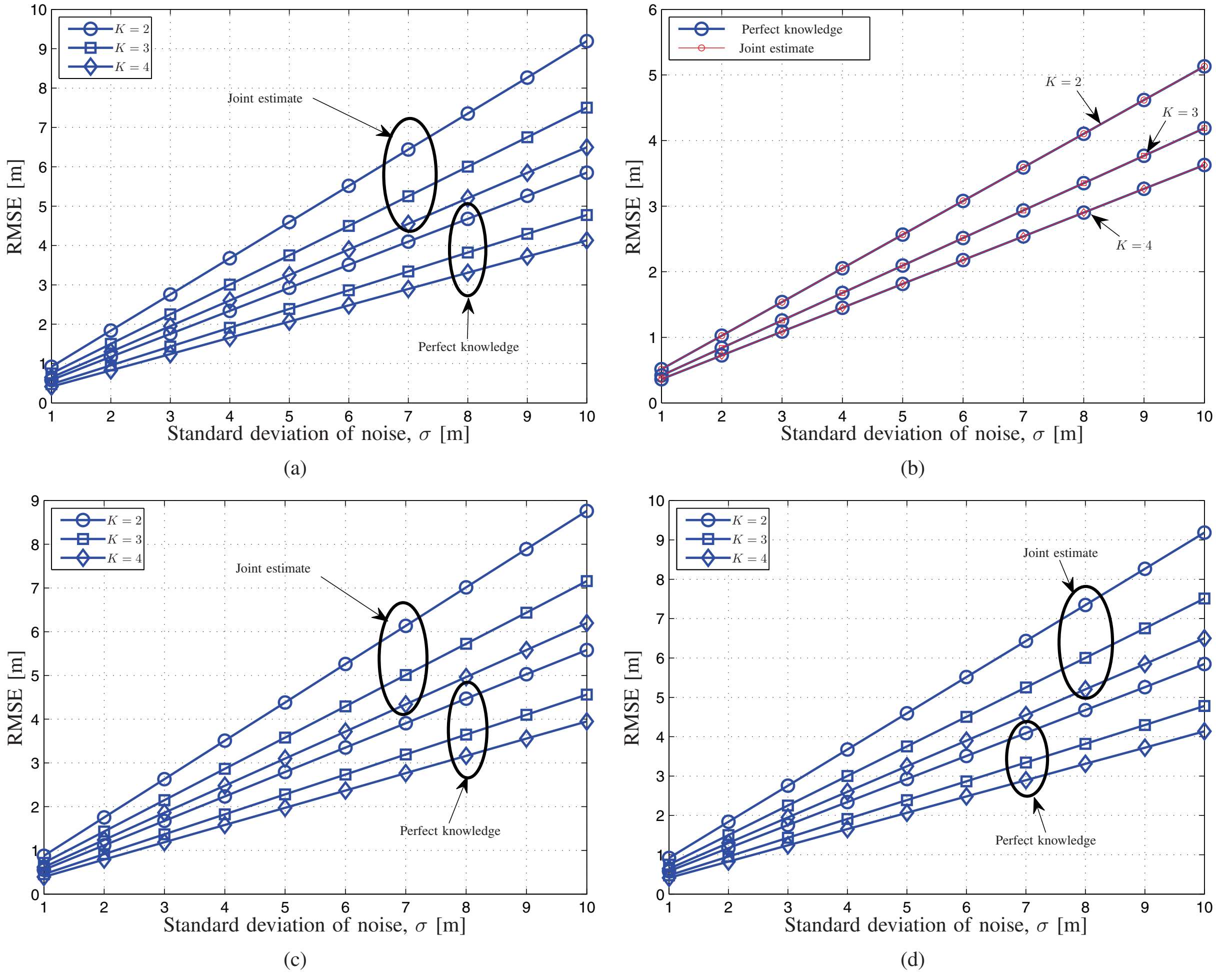

Fig. 4. CRLBs for various target nodes in two scenarios (joint estimate of the target position and the clock skew, and perfect knowledge of the clock skew) for (a) target node one, (b) target node two, (c) target node three, and (d) target node four.

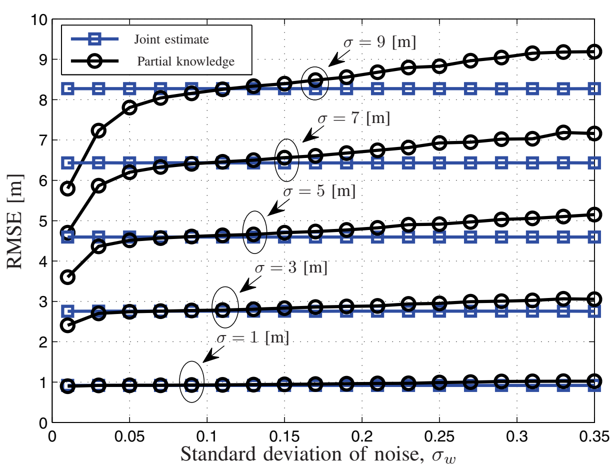

Fig. 6. CRLBs of target node node one position estimate when $K = 3$ for two scenarios: i) joint clock skew and position estimation, ii) partial knowledge of clock skew (in the form of a clock skew estimate) is available.

approach has better performance than the other one. From the figure, we can derive thresholds for σ_w and σ to specify when the joint estimation technique outperforms the other technique. For example, for target node one, when $\sigma_w \geq 0.15$ and $\sigma = 3$ meters, the joint estimation approach is superior.

C. Performance of Estimators

In this section, we evaluate the performance of the position estimation techniques developed in Section III and Section IV. To solve the MLE in (12), we use Matlab's function named *lsqnonlin* [32] initialized with the true value of the position and the clock skew or with the estimates from the SDP or LLS. To solve the SDP in (39), we employ the *CVX* toolbox [33]. The upper bound $\delta_{\max}$ in the SDP and the regularization parameter λ are set to 0.1 and 0.02, respectively. Fig. 7 shows the RMSEs of different approaches versus the standard deviation of the measurement noise. It is observed that the proposed estimators in the coarse estimation step can provide good initial points such that the MLE initialized with the coarse estimation step estimate (the SDP or LLS estimate) attains the CRLB. The figure also shows that the fine estimation step significantly improves the accuracy of the coarse estimate for both the SDP and LLS. In some scenarios, the SDP approach outperforms the LLS and in other scenarios the LLS has better performance compared to the SDP. For instance, the LLS approach for target one in Fig. 7(a) and Fig. 7(b) significantly outperforms the SDP and the LLS followed by the fine step estimation is very close to the CRLB. Note that the performance of the estimators can be improved by increasing the number of messages, K. From the figure it is observed that the behavior

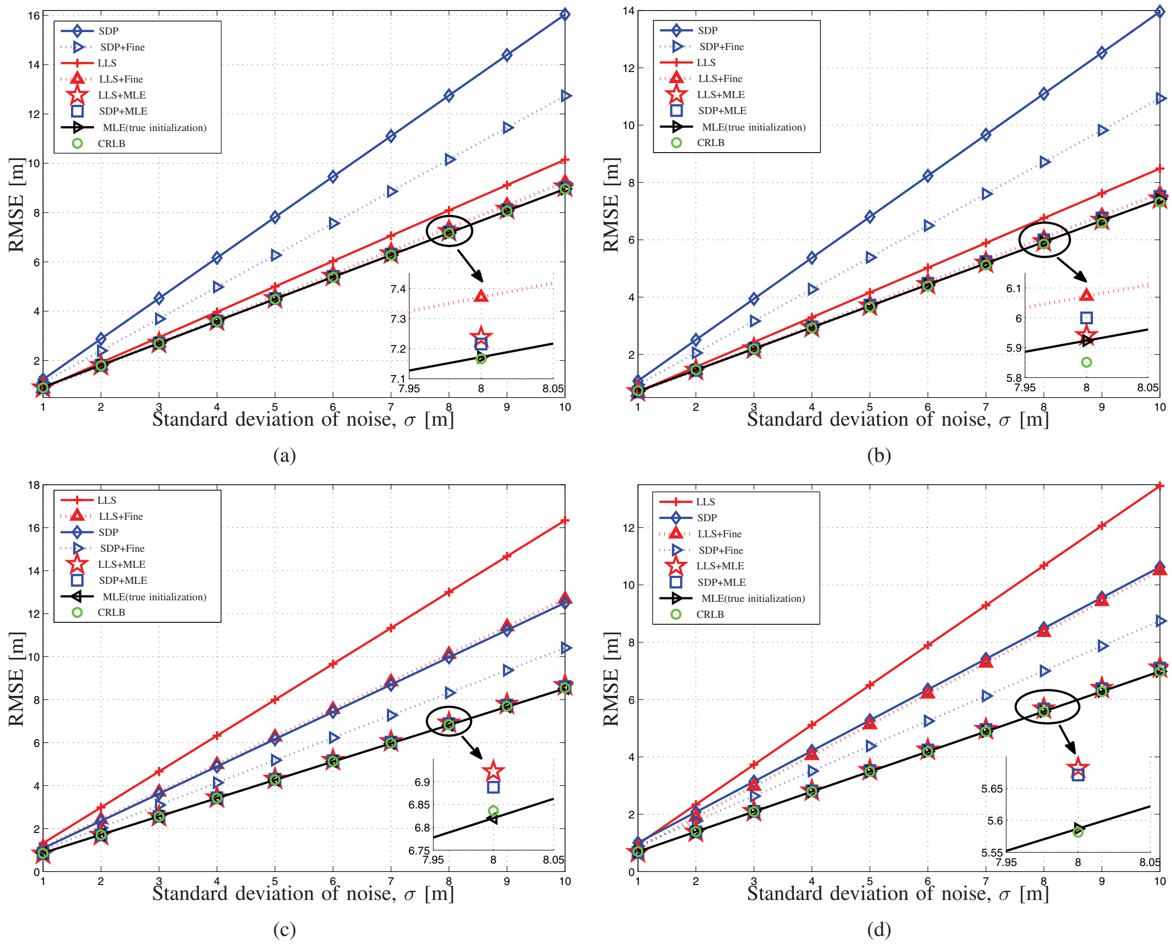

Fig. 7. RMSEs of various approaches for (a) target node one and $K = 2$, (b) target node one and $K = 3$, (c) target node three and $K = 2$, and (d) target node three and $K = 3$. Note the different scales on the vertical axis

of improvement can vary for different estimators. In fact, since we have derived the suboptimal estimators from the measurements using two different approaches, the relation between parameter K and the performance of the estimators can be different. It is also observed that the performance of the estimation depends on the geometry of the network. The effect of the geometry can be studied through the so-called geometric dilution of precision, e.g., see [1], which relates the position estimation error to the geometry of the network and the measurement errors. Finally, in Fig. 8, we plot the CDF of the position errors defined as $\|\hat{\mathbf{x}} - \mathbf{x}\|$, where $\hat{\mathbf{x}}$ is an estimate of the target position. For this figure, we set $K = 3$ and $\sigma = 2$ [m]. From the figure, we observe that the fine estimate considerably improves the coarse estimate most of the time and its performance is close to the MLE.

VI. Concluding Remarks

In this paper, we have studied the problem of self-positioning a single target node based on TDOA measurements when the local clock of the target node is unsynchronized. Although TDOA-based positioning is not sensitive to a clock offset, it suffers from another clock imperfection parameter, namely, the clock skew. To address this problem, we have considered a joint position and clock skew estimation technique and derived the MLE for this problem. Since the MLE is highly nonconvex, we have studied two suboptimal estimators that can be efficiently solved. Using relaxation and approximation techniques, we have derived two estimators based on semidefinite programming (SDP) and linear least squares (LLS) approximation. To further refine the estimates, we have linearized the measurements using the first order Taylor series around the SDP or LLS estimate to derive a linear model in which the estimation error can be approximated. To compare different approaches, we have derived the CRLBs for the problem when either no knowledge or partial knowledge of the clock skew is available. The simulation results show that the proposed techniques can attain the CRLB for sufficiently high signal-to-noise ratios.

References

[1] G. Mao and B. Fidan, *Localization Algorithms and Strategies for Wireless Sensor Networks*. Information Science Reference, 2009.

[2] Z. Sahinoglu, S. Gezici, and I. Guvenc, *Ultra-Wideband Positioning Systems: Theoretical Limits, Ranging Algorithms, and Protocols*. Cambridge University Press, 2008.

[3] N. Patwari, A. O. Hero, M. Perkins, N. S. Correal, and R. J. O'Dea, "Relative location estimation in wireless sensor networks," *IEEE Trans. Signal Process.*, vol. 51, no. 8, pp. 2137–2148, Aug. 2003.

[4] N. Patwari, J. Ash, S. Kyperountas, A. O. Hero, and N. C. Correal, "Locating the nodes: cooperative localization in wireless sensor network," *IEEE Signal Process. Mag.*, vol. 22, no. 4, pp. 54–69, July 2005.

[5] S. Gezici, "A survey on wireless position estimation," *Wireless Personal Commun.*, vol. 44, no. 3, pp. 263–282, Feb. 2008.

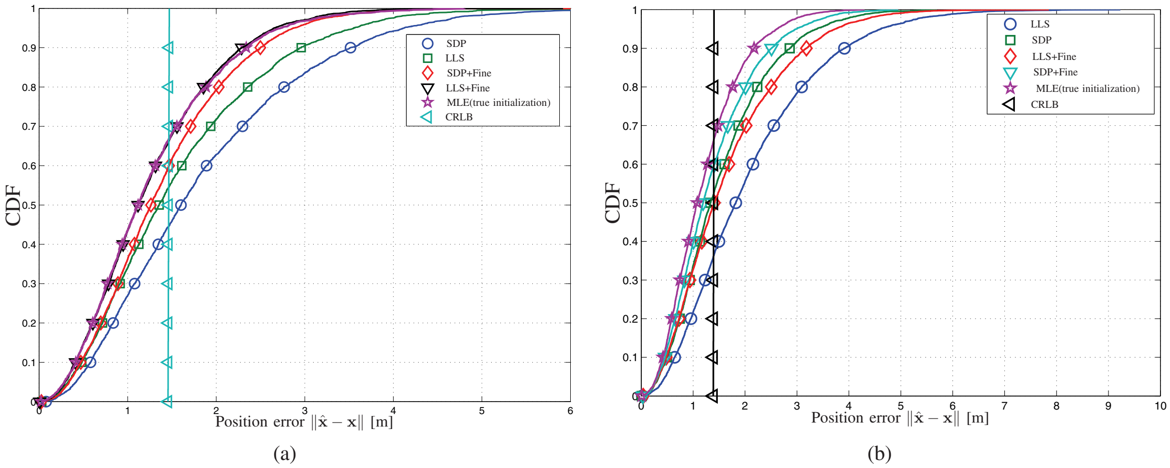

Fig. 8. CDFs of the position error for $\sigma = 2$ m and $K = 3$ for (a) target node one and (b) target node three.

[6] M. R. Gholami, E. G. Ström, and M. Rydström, "Indoor sensor node positioning using UWB range measurments," in *Proc. 2009 European Signal Process. Conf.*, pp. 1943–1947.

[7] Y. Wang, X. Ma, and G. Leus, "Robust time-based localization for asynchronous networks," *IEEE Trans. Signal Process.*, vol. 59, no. 9, pp. 4397–4410, Sept. 2011.

[8] M. R. Gholami, S. Gezici, and E. G. Ström, "A concave-convex procedure for TDOA based positioning," *IEEE Commun. Lett.*, 2013. Available: http://publications.lib.chalmers.se/records/fulltext/169494/local_169494.pdf

[9] N. M. Freris, S. R. Graham, and P. R. Kumar, "Fundamental limits on synchronizing clocks over networks," *IEEE Trans. Autom. Control*, vol. 56, no. 6, pp. 1352–1364, June 2011.

[10] Y.-C. Wu, Q. Chaudhari, and E. Serpedin, "Clock synchronization of wireless sensor networks," *IEEE Signal Process. Mag.*, vol. 28, no. 1, pp. 124–138, Jan. 2011.

[11] Q. M. Chaudhari, E. Serpedin, and K. Qaraqe, "Some improved and generalized estimation schemes for clock synchronization of listening nodes in wireless sensor networks," *IEEE Trans. Commun.*, vol. 58, no. 1, pp. 63–67, Jan. 2010.

[12] E. Serpedin and Q. M. Chaudhari, *Synchronization in Wireless Sensor Networks: Parameter Estimation, Performance Benchmarks and Protocols*. Cambridge University Press, 2009.

[13] Q. Chaudhari, E. Serpedin, and J. Kim, "Energy-efficient estimation of clock offset for inactive nodes in wireless sensor network," *IEEE Trans. Inf. Theory*, vol. 56, no. 1, pp. 582–596, Jan. 2010.

[14] J. Zheng and Y. Wu, "Joint time synchronization and localization of an unknown node in wireless sensor networks," *IEEE Trans. Signal Process.*, vol. 58, no. 3, pp. 1309–1320, Mar. 2010.

[15] Z. Sahinoglu and S. Gezici, "Ranging in the IEEE 802.15.4a standard," in *2006 IEEE Wireless Microwave Technol. Conf.*

[16] H. Fan and C. Yan, "Asynchronous differential TDOA for sensor self-localization," in *Proc. 2007 IEEE International Conf. Acoustics, Speech Signal Process.*, vol. 2, pp. 1109–1112.

[17] C. Yan and H. Fan, "Asynchronous differential TDOA for non-GPS navigation using signals of opportunity," in *Proc. 2008 IEEE International Conf. Acoustics, Speech Signal Process.*, pp. 5312–5315.

[18] ——, "Asynchronous self-localization of sensor networks with large clock drift," in *Proc. 2007 International Conf. Mobile Ubiquitous Syst.: Netw. Services*, pp. 1–8.

[19] M. R. Gholami, S. Gezici, and E. G. Ström, "Improved position estimation using hybrid TW-TOA and TDOA in cooperative networks," *IEEE Trans. Signal Process.*, vol. 60, no. 7, pp. 3770–3785, July 2012.

[20] I. Sari, E. Serpedin, K. Noh, Q. Chaudhari, and B. Suter, "On the joint synchronization of clock offset and skew in RBS-protocol," *IEEE Trans. Commun.*, vol. 56, no. 5, pp. 700–703, May 2008.

[21] M. R. Gholami, "Positioning algorithms for wireless sensor networks," Licentiate Thesis, Chalmers University of Technology, Mar. 2011. Available: http://publications.lib.chalmers.se/records/fulltext/138669.pdf

[22] Z. Sahinoglu, "Improving range accuracy of IEEE 802.15.4a radios in the presence of clock frequency offsets," *IEEE Commun. Lett.*, vol. 15, no. 2, pp. 244–246, Feb. 2011.

[23] S. M. Kay, *Fundamentals of Statistical Signal Processing: Estimation Theory*. Prentice-Hall, 1993.

[24] D. S. Bernstein, *Matrix Mathematics: Theory, Facts, and Formulas*, 2nd edition. Princeton University Press, 2009.

[25] L. Vandenberghe and S. Boyd, "Semidefinite programming," *SIAM Rev.*, vol. 38, no. 1, pp. 49–95, Mar. 1996.

[26] Z.-Q. Luo, W.-K. Ma, A. So, Y. Ye, and S. Zhang, "Semidefinite relaxation of quadratic optimization problems," *IEEE Signal Process. Mag.*, vol. 27, no. 3, pp. 20–34, May 2010.

[27] M. R. Gholami, S. Gezici, E. G. Ström, and M. Rydström, "Positioning algorithms for cooperative networks in the presence of an unknown turn-around time," in *Proc. 2011 IEEE International Workshop Signal Process. Advances Wireless Commun.*, pp. 166–170.

[28] S. Boyd and L. Vandenberghe, *Convex Optimization*. Cambridge University Press, 2004.

[29] M. R. Gholami, S. Gezici, E. G. Ström, and M. Rydström, "Hybrid TW-TOA/TDOA positioning algorithms for cooperative wireless networks," in *Proc. 2011 IEEE International Conf. Commun.*

[30] C. W. Ueberhuber, *Numerical Computation 1*. Springer-Verlag, 1997.

[31] G. Wang and K. Yang, "A new approach to sensor node localization using RSS measurements in wireless sensor networks," *IEEE Trans. Wireless Commun.*, vol. 10, no. 5, pp. 1389–1395, May 2011.

[32] The Mathworks Inc., 2012. Available: http://www.mathworks.com

[33] M. Grant and S. Boyd, "CVX: Matlab software for disciplined convex programming, version 1.21," Feb. 2011. Available: http://cvxr.com/cvx

Mohammad Reza Gholami (S'09) received the M.S. degree in communication engineering from University of Tehran, Iran in 2002. From 2002 to 2008, he worked as a communication systems engineer in industry on designing receivers for different digital transmission systems. Currently, he is working toward the Ph.D. degree at Chalmers University of Technology. His main interests are statistical inference, convex optimization techniques for signal processing and digital communications, cooperative and noncooperative positioning approaches, and network wide synchronization techniques for wireless sensor networks.

Sinan Gezici (S'03, M'06, SM'11) received the B.S. degree from Bilkent University, Turkey in 2001, and the Ph.D. degree in Electrical Engineering from Princeton University in 2006. From 2006 to 2007, he worked at Mitsubishi Electric Research Laboratories, Cambridge, MA. Since 2007, he has been with the Department of Electrical and Electronics Engineering at Bilkent University, where he is currently an Associate Professor. Dr. Gezici's research interests are in the areas of detection and estimation theory, wireless communications, and localization systems. Among his publications in these areas is the book Ultra-wideband Positioning Systems: Theoretical Limits, Ranging Algorithms, and Protocols (Cambridge University Press, 2008). Dr. Gezici is an associate editor for IEEE Transactions on Communications, IEEE Wireless Communications Letters, and Journal of Communications and Networks..

Erik G. Ström (S'93–M'95–SM'01) received the M.S. degree from the Royal Institute of Technology (KTH), Stockholm, Sweden, in 1990, and the Ph.D. degree from the University of Florida, Gainesville, in 1994, both in electrical engineering. He accepted a postdoctoral position at the Department of Signals, Sensors, and Systems at KTH in 1995. In February 1996, he was appointed Assistant Professor at KTH, and in June 1996 he joined Chalmers University of Technology, Göteborg, Sweden, where he is now a Professor in Communication Systems since June 2003. Dr. Ström currently heads the Division for Communications Systems, Information Theory, and Antennas at the Department of Signals and Systems at Chalmers and leads the competence area Sensors and Communications at the traffic safety center SAFER, which is hosted by Chalmers. His research interests include signal processing and communication theory in general, and constellation labelings, channel estimation, synchronization, multiple access, medium acccess, multiuser detection, wireless positioning, and vehicular communications in particular. Since 1990, he has acted as a consultant for the Educational Group for Individual Development, Stockholm, Sweden. He is a contributing author and associate editor for Roy. Admiralty Publishers FesGas-series, and was a co-guest editor for the PROCEEDINGS OF THE IEEE special issue on Vehicular Communications (2011) and the IEEE JOURNAL ON SELECTED AREAS IN COMMUNICATIONS special issues on Signal Synchronization in Digital Transmission Systems (2001) and on Multiuser Detection for Advanced Communication Systems and Networks (2008). Dr. Ström was a member of the board of the IEEE VT/COM Swedish Chapter 2000–2006. He received the Chalmers Pedagogical Prize in 1998 and the Chalmers Ph.D. Supervisor of the Year award in 2009.